

**BELGIAN FEDERAL SCIENCE POLICY
RESEARCH FELLOWSHIPS
(NON – EU POSTDOCS)**

Nataliia Guzenko, Dr
01.03.2011 – 31.05.2012

Project leader: Colonel **Peter LODEWYCKX, Dr Ir**
Royal Military Academy – Dept of Chemistry – Renaissancelaan 30 – B1000 Brussel
Phone: +32-2-742.63.00 Fax: +32-2-742.63.02
E-mail: Peter.Lodewyckx@rma.ac.be

Final report

Modeling the water vapour isotherm in order to understand the influence of pre-adsorbed water on filter breakthrough performance.

1 Introduction

The adsorption of water molecules on carbon adsorbents has a number of peculiarities compared with the adsorption of nonpolar substances [1-3]. Regularities and features of water vapour adsorption on carbon adsorbents are determined, e.g. a tendency of the polar water molecules to form hydrogen bonds at relatively weak dispersion interactions with the carbon surface [1, 2]. One of the distinctive properties, which largely determines the application of carbon adsorbents, is their relative hydrophobicity [4-6]. However, depending on porosity and chemical state of the surface, which can be changed during extended storage or long-term use of the adsorbents, the humidity of the environment can significantly affect the adsorption capacity of carbon adsorbents to certain substances [7, 8]. In connection with this, the investigation of the features and particularities of water vapour adsorption and the modeling of the water vapour isotherm in order to understand the influence of pre-adsorbed water on carbon filter breakthrough performance assume an important practical significance.

For the comprehension of the water vapour adsorption mechanism, first of all, it is necessary to know the characteristics of the pore structure of the investigated activated carbon as well as the chemical state of the surface and the nature of the primary adsorption centres [1, 5, 9-12].

2 Experimental

Materials. Three pairs of activated carbons (Norit, the Netherlands) with similar values of surface area but different pore size distribution (volume of micropores versus mesopores) have been chosen for the investigation in this study.

Methods. *Sorption of Nitrogen and Carbon Dioxide.* The pore structure characteristics of the examined materials were determined by employing physical adsorption methods (Nitrogen adsorption at 77 K and Carbon dioxide at 273 K). The adsorption isotherms were measured on an Autosorb-1 (Quantachrome instruments, USA). Before to adsorption, the samples were outgassed at 100°C during 24 hours *in vacuo* (10^{-5} - 10^{-6} Torr). The build-in Quantachrome software (AS1Win, Version 1.53) was used for carrying out of the data acquisition and computing.

Thermogravimetric Analysis (TGA). TGA experiments were carried out with a Mettler Toledo TGA/SDTA 851 Star system thermobalance (Switzerland). In a typical analysis, about 20 mg of sample was heated in an alumina pan at a heating rate of 10 °C/min up to 1050 °C in an Ar (or N₂) atmosphere, flowing at 60 cm³/min.

Temperature-Programmed Desorption Mass-Spectrometry (TPD-MS). Gases and vapours which evolved during the TGA decomposition were monitored continuously by using a Pfeiffer Vacuum Introduces ThermoStar™ Gas Analysis System (Germany). Intensity of evolved mass (A)

as well as concentrations (%) of CO, CO₂ and H₂O in an Ar and N₂ flow, time and temperature are recorded by a computerized data acquisition system.

X-ray Photoelectron Spectroscopy. The XPS measurements were carried out on a Clam 2 (XPS) hemispherical electron energy analyzer and a XR3E2 (VG Microtech) twin anode X-ray source, using nonmonochromatic Mg K_α (1253.6 eV) radiation. The base pressure of the analysis chamber was 5·10⁻⁷ Pa. Wide scan spectra were recorded in the 0-1000 eV binding energy range at 50 eV pass energy for all samples while the high resolution (detailed) spectra of the main constituent elements (C 1s and O 1s signals) were recorded by 0.05 eV steps at 20 eV pass energy. Peak area intensity data were obtained after background subtraction. The C 1s and O 1s lines of the high resolution spectra were decomposed into Gaussian components by the peak synthesis method.

Sorption of Water. Water adsorption isotherms were determined at 293 K using Hydrosorb (Quantachrome instruments, USA). Samples were evacuated at 150 °C and 10⁻⁶ Torr for 12 hours prior to adsorption measurements.

3 Results and Discussion

Determination of the pore structure characteristics of activated carbons. The isotherms of the nitrogen adsorption on the activated carbon samples have forms similar to a type IV isotherm (IUPAC) (fig. 1) [6, 13]. The steep raise in the first part of the isotherms indicates the presence of a considerable quantity of micropores. The narrow hysteresis loops between the adsorption and desorption branches observed at relative pressures $p/p_0 > 0.5$, which are observed for samples 110362, 110361, 110680, can be explained by capillary condensation of the adsorbate into the lower limits of the mesopore range (2-50 nm) [14, 15]. The increased slope at high relative pressures indicates the existence of an external surface. The calculations of the specific surface area, the pore volume, the average pore width, and the pore size distribution of the activated carbons were carried out by using the DR, DFT and BJH methods. The comparative data of different methods are presented in Table 1 and 2.

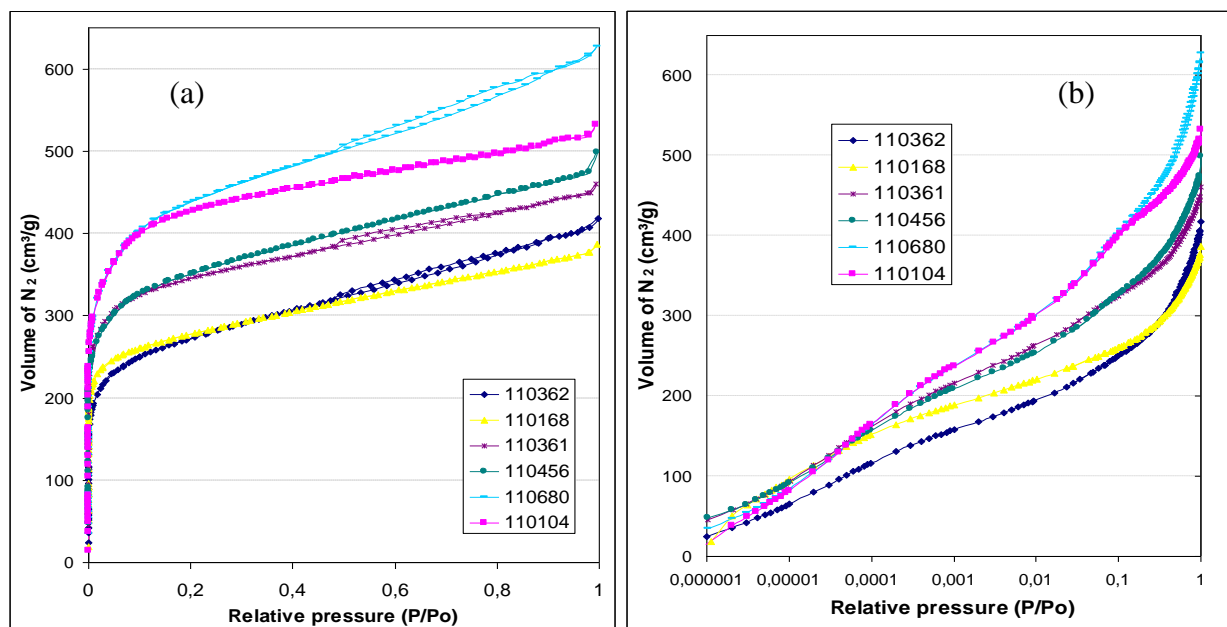


Fig. 1. Adsorption isotherms of N₂ measured at 77 K on activated carbon samples: linear (a) and logarithmic scale (b).

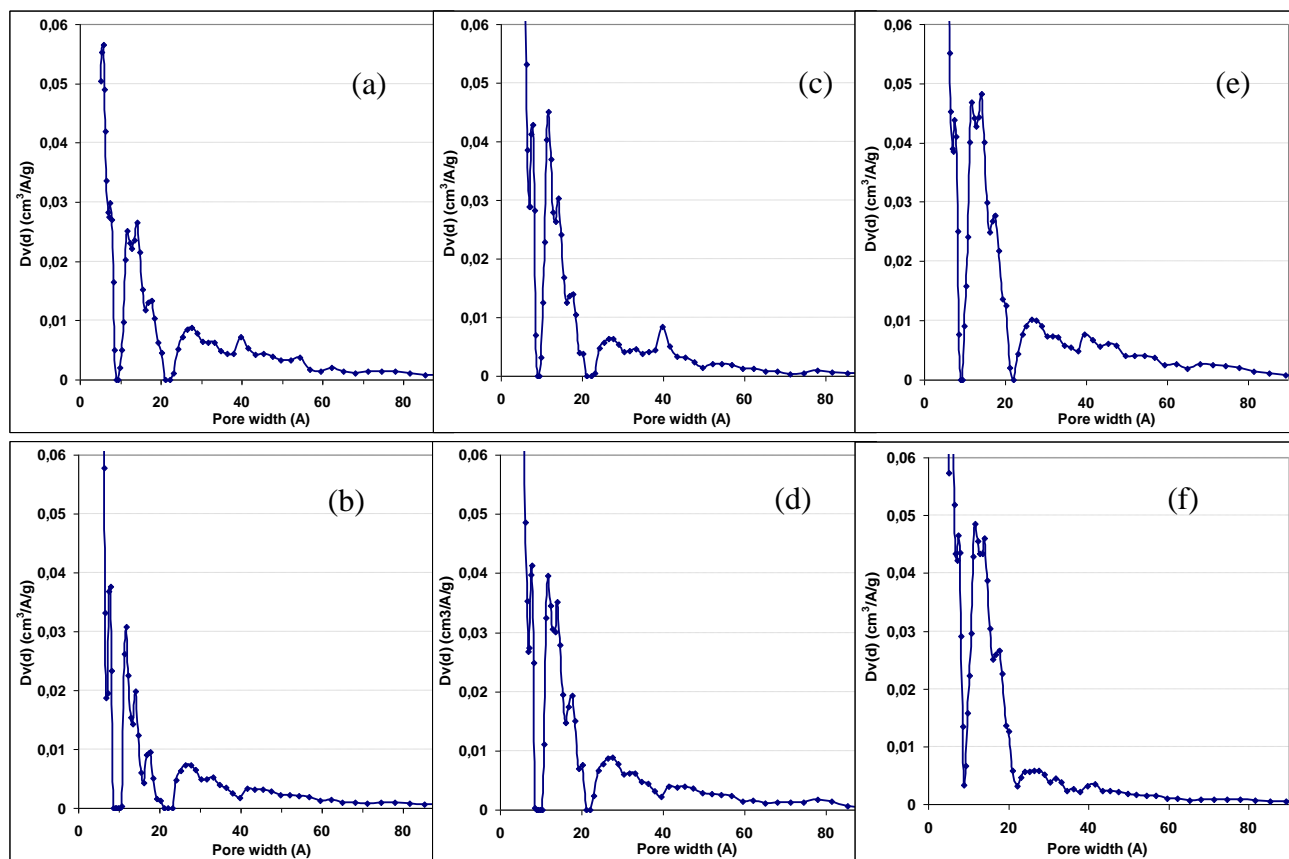
Analysis of the data given in Tables 1 and 2 shows that the calculation of structural parameters of the samples such as total pore volumes, micropore and mesopore volumes by using of different methods (DR, DFT and BJH) gives similar results for each carbon. Concurrently each pair of activated carbons with close values of surface areas have approximate the same micropore volumes (and, probably, microporous structures), but different amounts of mesopores and, as a result, different total pore volume.

Table 1. Structural characteristics of the activated carbons derived from N₂ adsorption isotherms.

Sample code	S _{BET} (m ² /g)	Total pore volume (p/p ₀ =0.98) (cm ³ /g)	S _{micropore} DR (m ² /g)	V _{micropore} DR (cm ³ /g)	Adsorption energy (E ₀) (kJ/mol)	Average pore width (nm)	V _{mesopore} = col 3 – col 5 (cm ³ /g)
1	2	3	4	5	6	7	8
110362	997	0.63	973	0.35	19.3	1.35	0.28
110168	1029	0.56	1056	0.38	22.8	1.14	0.21
110361	1295	0.70	1307	0.47	19.9	1.31	0.23
110456	1296	0.74	1257	0.45	20.0	1.30	0.29
110680	1628	0.95	1546	0.55	17.9	1.45	0.40
110104	1604	0.81	1532	0.55	18.1	1.44	0.26

Table 2. Structural characteristics of the activated carbons derived from N₂ adsorption isotherms.

Sample code	Pore volume DFT (cm ³ /g)	V _{micropore} DFT (<20 Å) (cm ³ /g)	V _{mesopore} DFT = col 2 – col 3 (cm ³ /g)	Cumulative desorption surface area BJH (m ² /g)	V _{mesopore} BJH (cm ³ /g)
1	2	3	4	5	6
110362	0.58	0.33	0.25	729	0.32
110168	0.54	0.36	0.18	508	0.23
110361	0.64	0.46	0.19	741	0.25
110456	0.68	0.45	0.23	899	0.29
110680	0.88	0.55	0.33	1291	0.41
110104	0.73	0.56	0.17	1195	0.23

Fig. 2. Pore size distribution of activated carbon samples 110362 (a), 110168 (b), 110361 (c), 110456 (d), 110680 (e), and 110104 (f) obtained from the DFT analysis of N₂ isotherms.

“Mesoporous” samples, which give hysteresis loops between adsorption and desorption branches of nitrogen isotherms, in general, have bigger mesopore volumes, than “microporous” samples. But this rule doesn’t work in case of carbon pair of 110361 and 110456 (see table 1 and 2). The main distinction in pore structures of the “mesoporous” (110362, 110361, 110680) and “microporous” samples (110168, 110456, 110104), which can be observed by the pore size distribution analysis (DFT), is the existence of additional porosity in range of pore width 35-45 Å (fig. 2).

Nitrogen adsorption results agree with Carbon dioxide analysis at 273 K in the range of small micropores (where CO₂ adsorption is most applicable) that can testify, in addition, to the existence of ultramicropores in the tested materials (Fig. 3, Table 3) [16, 17].

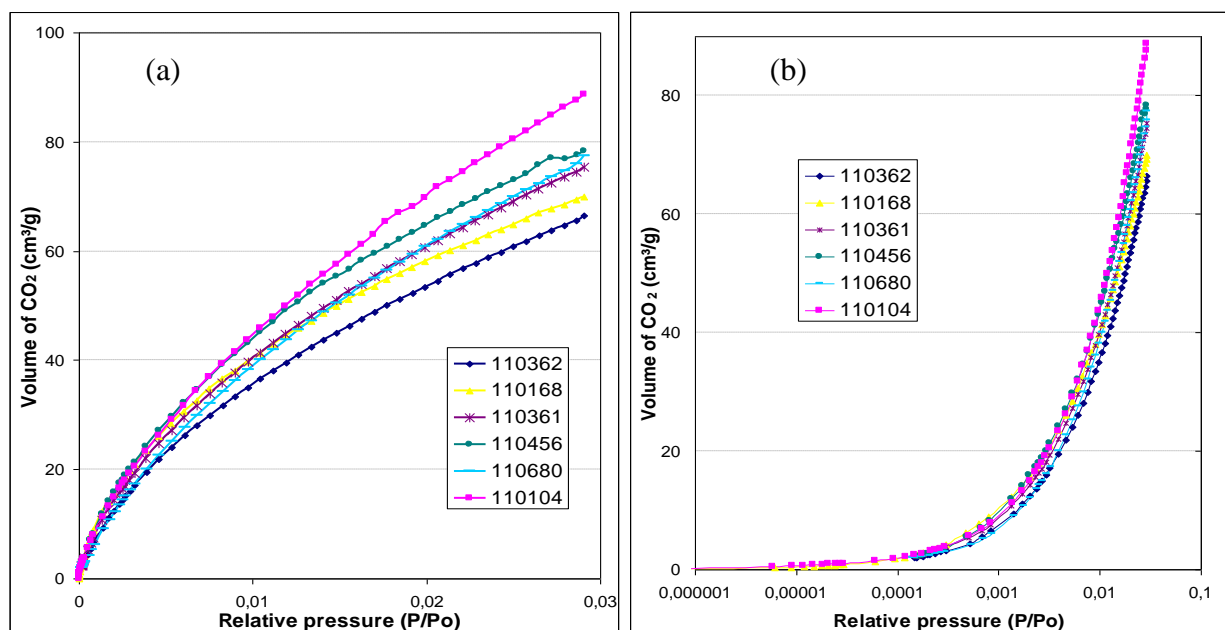


Fig. 3. Adsorption isotherms of CO₂ at 273 K on Norit activated carbons: lineal (a) and logarithmic scale (b).

Table 3. Structural characteristics of the activated carbons derived from Carbon dioxide adsorption isotherms.

Sample code	S micro pore DR (m ² /g)	V micro pore DR (cm ³ /g)	Adsorption energy (E ₀) (kJ/mol)	Average pore width (nm)	Pore volume (micro) DFT (<14.75 Å) (cm ³ /g)
110362	895	0.31	17.22	1.51	0.25
110168	860	0.30	18.28	1.42	0.23
110361	1030	0.36	17.11	1.52	0.29
110456	1011	0.35	17.80	1.46	0.26
110680	1130	0.39	16.45	1.58	0.33
110104	1337	0.47	16.25	1.60	0.32

The investigation of activated carbon surface chemistry by Thermogravimetric Analysis and Temperature-Programmed Desorption Mass-Spectrometry techniques. In order to describe the surface chemistry of the activated carbon samples, their thermal regenerations were determined by both Thermogravimetric Analysis (TGA) and Temperature-Programmed Desorption Mass-Spectrometry (TPD-MS) techniques.

The shapes of the TGA curves of the used activated carbons show that the evaporation of physically adsorbed water vapours is generally finished at 120 -150 °C (Fig. 4, 5). Furthermore shifts of peak maximum of water evaporation to lower temperature are observed with the increase of specific surface area (micropore volume) of the samples (Fig. 4 b, 5). The weight losses in all

range of temperatures higher than 150 °C testify to a multi-step decomposition of the carbons with formation of gaseous reaction products (Table 4). Concurrently for the mesoporous samples (110362, 110361, 110680) are observed more significant decomposition peaks with the maximum at 660-690 °C, that indicate the presence of addition functional groups on the surface of these carbons (Fig. 4 b).

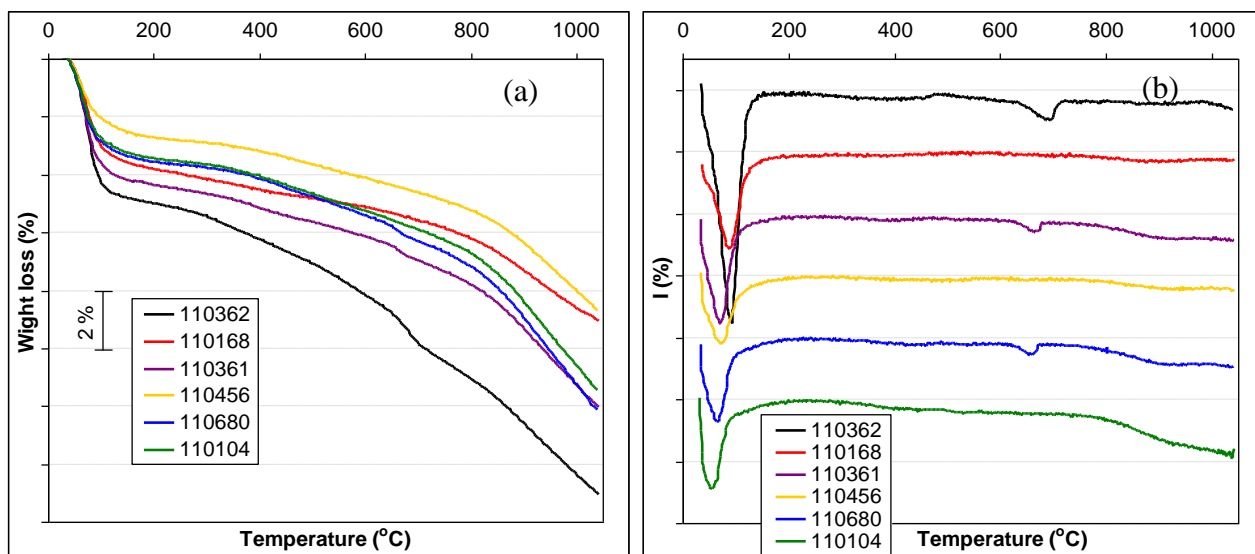


Fig. 4. TG (a) and DTG (b) curves of the carbons in Ar atmosphere.

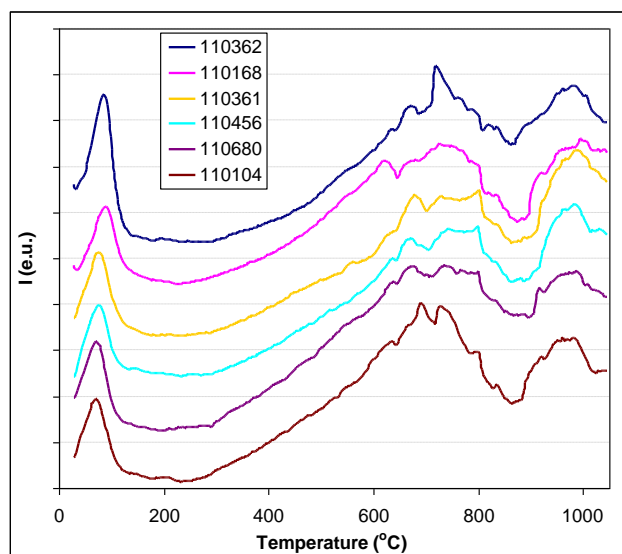


Fig. 5. DTA curves of the carbons in N₂ atmosphere.

The TPD spectra of 18, 28 and 44 masses have quite similar forms and peak positions for all examined activated carbons that testify to sufficiently close compositions of their surfaces. H₂O desorption maxima in the TPD spectra can be detected at temperatures below 100 °C, where loosely bounded physically adsorbed molecules of water are desorbed [18]. This indicates that water is not a product of the decomposition of surface hydroxyl groups in the case of the samples (Fig. 6).

The sources of the low-temperature CO₂ desorption might be sites with carboxyl groups, which are less stable [19]. Carbon dioxide evolution at higher temperatures (400-700 °C) can be explained by the presence of very stabilised carboxylic groups, anhydrides or lactones [18-20]. The characteristic peaks centred at 670-690 °C, which are observed on DTG and MS curves of the mesoporous samples (110362, 110361, 110680), could be identified as the decomposition of calcium carbonate (as it will be shown by the XPS method the presence of calcium is a distinctive feature of these carbons) [21, 22]. In addition CO₂ desorption was still significantly high at the

termination point (1050 °C) for all samples, so some oxides remained on the surface at the end of the TPD run (Fig. 7). The CO₂ desorption at these temperatures may be assigned to the presence of acid-anhydride and/or lactone groups [18].

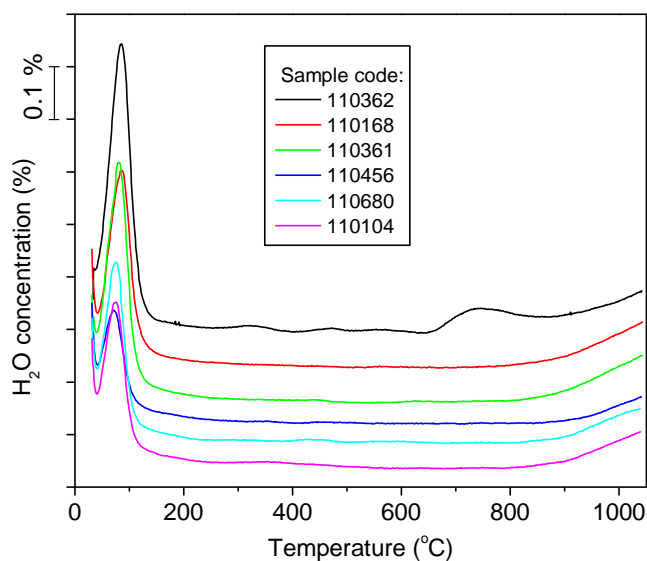


Fig. 6. H₂O concentration ($m/z = 18$) as a function of temperature in Ar flow for activated carbon samples (TPD-MS data).

The profiles of CO₂ have a wide bands ranging from 250 up to 1050 °C with a few maxima near 120, 400, 520, 670-690 and 900-1000 °C (Fig. 7).

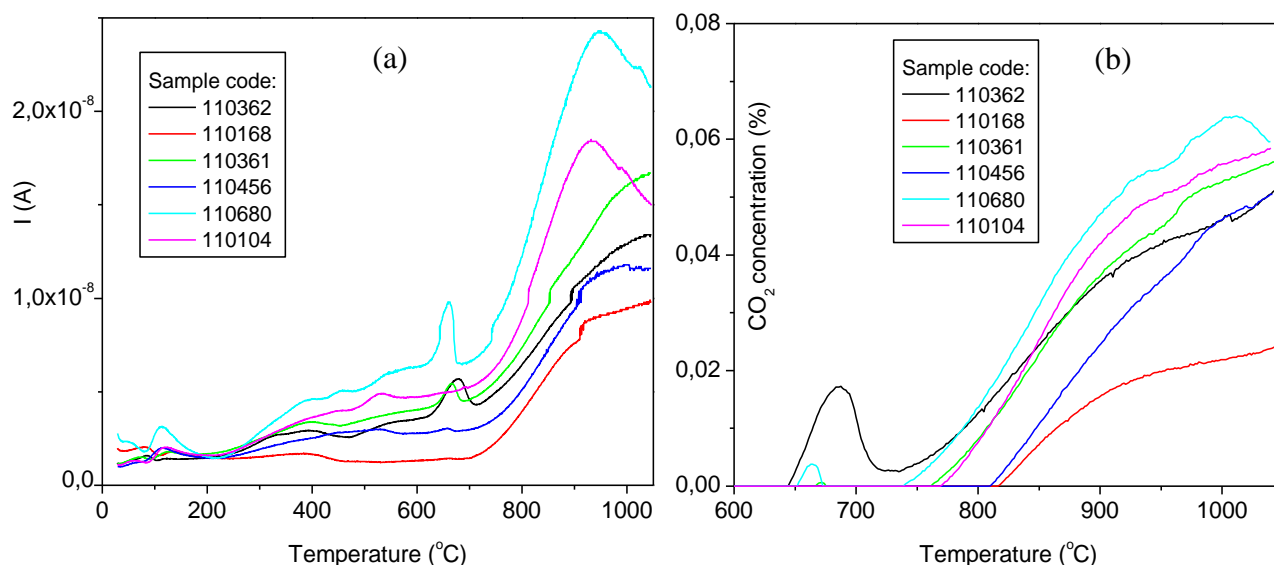


Fig. 7. TPD-MS spectra (a) and CO₂ concentration ($m/z = 44$) as a function of temperature in Ar flow for activated carbon samples (TPD-MS data) (b).

CO evolution begins at higher temperatures and has the main maxima at 900 °C (Fig. 8). In this temperature range (700–980 °C) phenol, ether, carbonyl and quinone groups can be decomposed with CO emission [18-20]. The CO desorption from the sample at temperatures above 1000 °C may be due to the presence of carbonyl, pyrone groups [20] and/or to the decomposition of semiquinone groups [18].

In order to compare all the results quantitatively, the amounts of desorbed H₂O, CO and CO₂ for each sample were calculated. The calibration method was based on the use of suitable salts of K₂C₂O₄·H₂O and CaCO₃ for the calibration of CO (H₂O) and CO₂ respectively [18]. The results were obtained in mole of the gases desorbed from 1.00 g of each samples (Table 4).

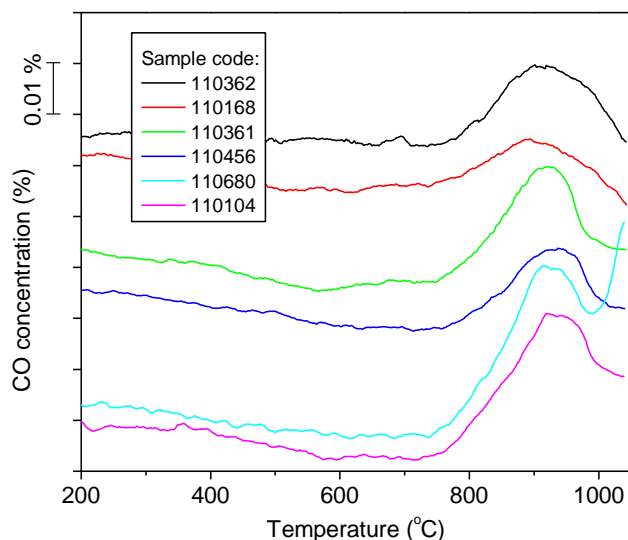


Fig. 8. CO concentration ($m/z = 28$) as a function of temperature in Ar flow for activated carbon samples (TPD-MS data).

The data given in table 4 indicate that mesoporous samples (110362, 110361, 110680) consist bigger total amounts of the surface oxygen complexes, which desorbed as CO and CO₂ groups at the heating to 1050 °C, than microporous carbons. These data are agreed with the results of TG analysis.

Table 4. TGA and TPD-MS experiment results.

Sample code	TGA data			TPD-MS data						
	Weight loss (wt.%)			C _{H2O} (mmol/g)	C _{H2O} (wt.%)	C _{CO} (mmol/g)	C _{CO2} (mmol/g)	C _{CO} (wt.%)	C _{CO2} (wt.%)	C _(CO+CO2) (wt.%)
	total	30-120°C (H ₂ O _{des.})	120-1050 °C							
110362	15.06	4.62	10.44	2.70	4.86	0.42	1.72	1.18	7.57	8.75
110168	9.05	3.32	5.73	1.92	3.46	0.29	0.63	0.81	2.79	3.61
110361	12.04	3.95	8.09	2.12	3.82	0.61	1.62	1.71	7.12	8.84
110456	8.68	2.28	6.40	1.36	2.45	0.40	1.16	1.11	5.11	6.22
110680	12.14	3.13	9.01	1.75	3.14	0.91	2.02	2.55	8.88	11.43
110104	11.46	2.99	8.47	1.73	3.11	0.56	1.73	1.57	7.59	9.17

Characterization of the surfaces of the carbon materials by the method of X-ray Photoelectron Spectroscopy. The surface compositions and chemical state of the activated carbon samples were also studied by the method of X-ray Photoelectron Spectroscopy (XPS).

The wide scan spectra of the activated carbons show the existence, except two main constituent elements (carbon C 1s and oxygen O 1s), also signals of K 2s, F 1s, and Ca 2p on the surface layers of the samples. Contents of the elements on the surface of the investigated carbons are given in Table 5. It should be noted that the presence of Ca is specific feature of the mesoporous samples. Moreover the mesoporous carbons have higher degrees of surface oxidation (oxygen contents) than microporous samples.

Six types of carbon atoms can be found in the surface layers of the investigated carbon materials by resolving of each high resolution C 1s spectrum into peaks (Fig. 9). The values of binding energy (EB) in C 1s spectra were [23-30] EB = 284.2-284.4 eV (peak I), which can be refer to amorphous graphitic carbon; EB = 285.1-285.3 eV (peak II) – carbon atom in composition of C-H, C-H₂-groups, hydrocarbons; EB = 286.0-286.2 eV (peak III) – carbon, which present in alcohol (C-O-H), phenolic or ether (C-O-C) groups; EB = 287.7-287.9 eV (peak IV) – carbonyl (C=O), quinone groups or F-bounded carbon (C-F); EB = 289.9-290.1 eV (peak V) – carboxyl (C(O)-OR), ester groups (O-C=O) or carbon in carbonate (O-C(O)-O); and EB = 292.3-292.5 eV (peak VI) – 2F-bounded carbon (-CH₂-CF₂-) or C in polytetrafluoroethylene (-CF₂-CF₂-) (Table 6).

Table 5. Composition of surface layers of activated carbons from the survey XPS spectra.

Sample code	C total area	O total area	Contents of element, % atomic				
			C 1s	O 1s	K 2s	F 1s	Ca 2p
110362	4694.1	788.4	82.8	14.1	0.8	0.3	2.0
110168	4166.1	367.3	90.4	8.0	0.9	0.8	0.0
110361	3862.3	486.8	87.1	10.7	0.9	0.4	0.9
110456	4524.2	339.4	91.9	6.9	0.7	0.4	0.2
110680	4423.0	535.0	88.2	9.7	1.1	0.2	0.8
110104	3959.8	361.1	88.5	9.6	1.3	0.5	0.0

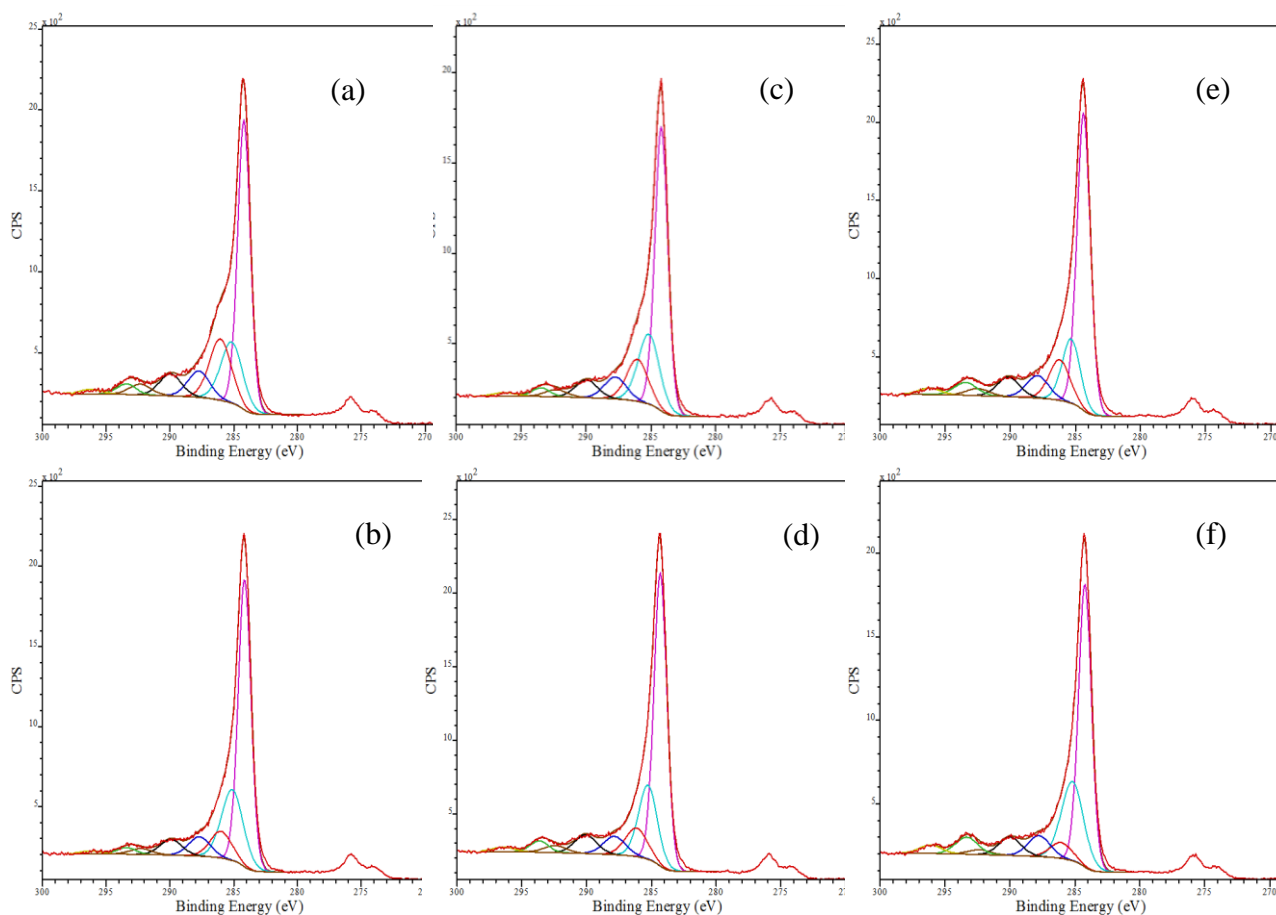


Fig. 9. X-ray photoelectron spectra showing the C 1s core level in activated carbon for samples 110362 (a), 110168 (b), 110361 (c), 110456 (d), 110680 (e), and 110104 (f).

Table 6. Peak positions and quantitative distributions of C-structures on the surfaces of activated carbons from C 1s spectra.

Sample code	Peak positions [eV]						% of the components (by element)					
	I	II	III	IV	V	VI	I	II	III	IV	V	VI
110362	284.2	285.2	286.1	287.7	290.0	292.3	48.1	17.4	17.5	7.6	6.3	3.1
110168	284.2	285.1	286.0	287.7	289.9	292.3	54.9	23.0	8.7	6.3	5.1	1.9
110361	284.2	285.2	286.0	287.7	290.0	292.3	51.8	20.9	12.7	6.9	5.5	2.2
110456	284.3	285.3	286.2	287.8	290.1	292.4	55.8	20.4	9.3	6.0	6.1	2.3
110680	284.4	285.3	286.2	287.9	290.1	292.5	56.1	16.4	12.0	7.1	6.2	2.3
110104	284.2	285.2	286.1	287.8	290.0	292.4	54.3	26.0	5.1	6.9	6.1	1.6

The data of XPS analysis testify that the mesoporous carbons (110362, 110361, 110680) have in consist of their surfaces relatively more intensive peaks with values of binding energy $EB = 286.0-286.2$ eV (peak III), which can be identified as those originating from alcohol or ether groups, and less intensive peaks with $EB = 285.1-285.3$ eV (peak II), which correspond to hydrocarbons.

Four types of oxygen were distinguished in the O 1s spectra (Fig. 10). Peak I at lower binding energies ($EB = 530.4-531$ eV) is most likely corresponding to non-bridging oxygen in -O-Me (where Me = K or Ca) [23, 24, 29]; peak II ($EB = 531.8-532.6$ eV) could be ascribed to oxygen atom in carbonyl functional groups ($C=O$, $O-C=O$); peak III ($EB = 533.4-534$ eV) to C-O oxygen in ether ($C-O-C=O$), anhydride, lactone or carboxylic acids [23, 24]; and peak IV ($EB = 535.2-536.1$ eV) to chemisorbed O_2 , adsorbed or bulk water [25-28], respectively (Table 7).

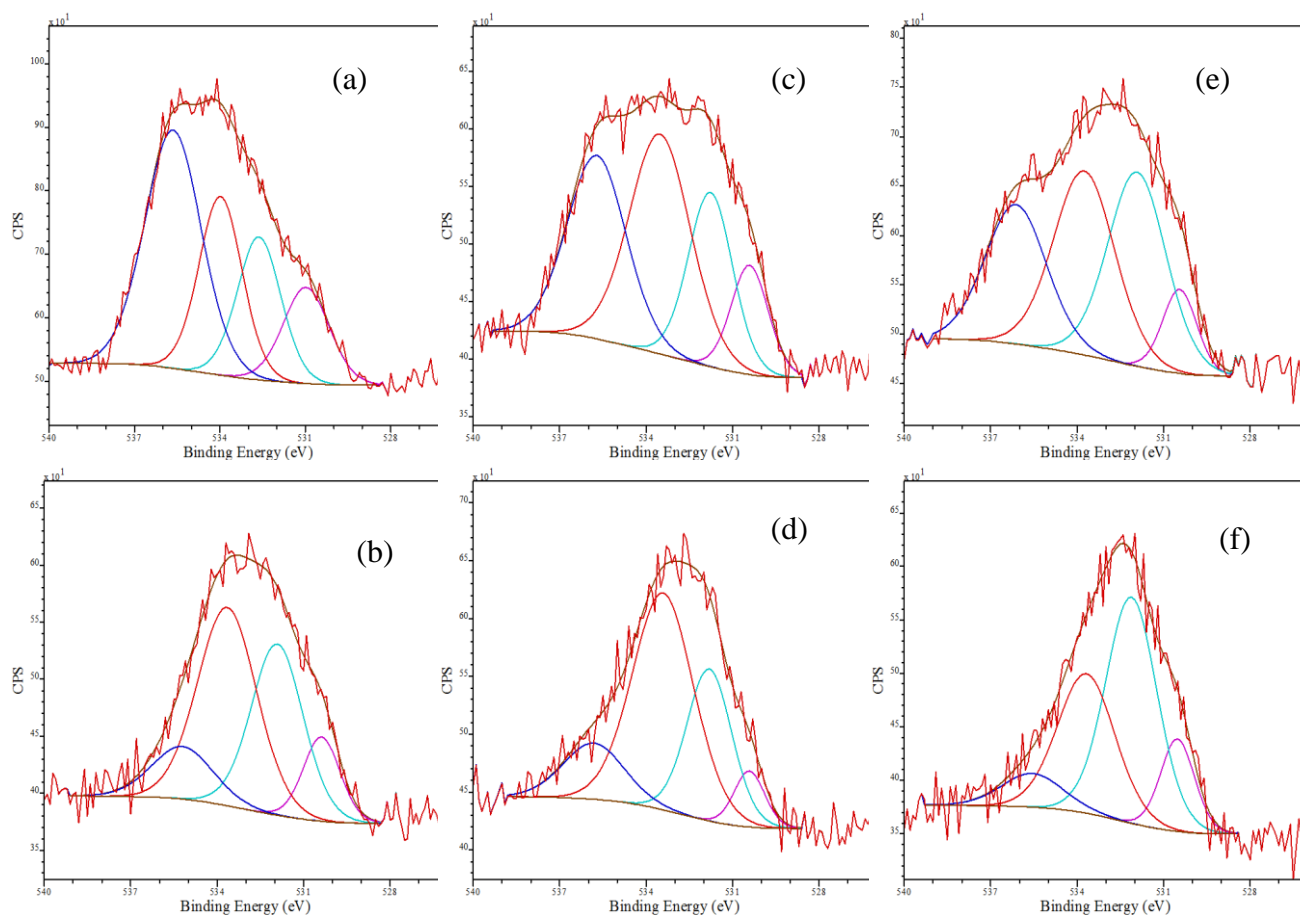


Fig. 10. X-ray photoelectron spectra showing O 1s core level in activated carbon for samples 110362 (a), 110168 (b), 110361 (c), 110456 (d), 110680 (e), and 110104 (f).

Table 7. Peak positions and quantitative distributions of O-structures on the surfaces of activated carbons from O 1s spectra.

Sample code	Peak positions [eV]				% of the components (by element)			
	I	II	III	IV	I	II	III	IV
110362	531.0	532.6	534.0	535.6	13.9	19.6	24.2	42.3
110168	530.4	531.9	533.6	535.2	11.5	33.1	43.5	11.9
110361	530.4	531.8	533.5	535.7	11.2	21.4	37.3	30.0
110456	530.4	531.8	533.4	535.8	6.7	27.1	52.6	13.6
110680	530.4	531.9	533.8	536.1	8.4	33.3	33.1	25.1
110104	530.5	532.1	533.7	535.5	12.7	46.8	32.3	8.3

Concurrently microporous samples (110168, 110456, 110104) have relatively bigger peaks with binding energy $EB = 531.8\text{--}532.6$ eV (peak II), which are probably due to carbonyl, and with $EB = 533.4\text{--}534$ eV (peak III) due to ether, anhydride, lactone or carboxylic acids, whereas the main distinction of mesoporous carbons are more intensive peaks with $EB = 535.2\text{--}536.1$ eV (peak IV), which are probably related to adsorbed or bulk water.

A detailed comparison of the techniques which have been employed for the surface characterization of the used sorbents (TGA, TPD-MS and XPS) show that XPS method gives higher values of total contents of oxygen on activated carbon surfaces (Fig. 11). This can be explained by the fact that we didn't have complete removal of organics from the activated carbon surfaces at the end of TPD-experiments as it has already noted above. Another reason for the phenomenon, which is observed, may be that there are oxygen-contents groups on the surfaces of the investigated carbons, which can't be removed as CO or CO₂ during the TPD-experiments (for example oxygen in inorganic oxides). Nevertheless, the change tendency of the total oxygen contents in the investigated activated carbons (higher for the mesoporous samples in each pair of carbons with close values of surface areas) remains essentially the same regardless of the research method.

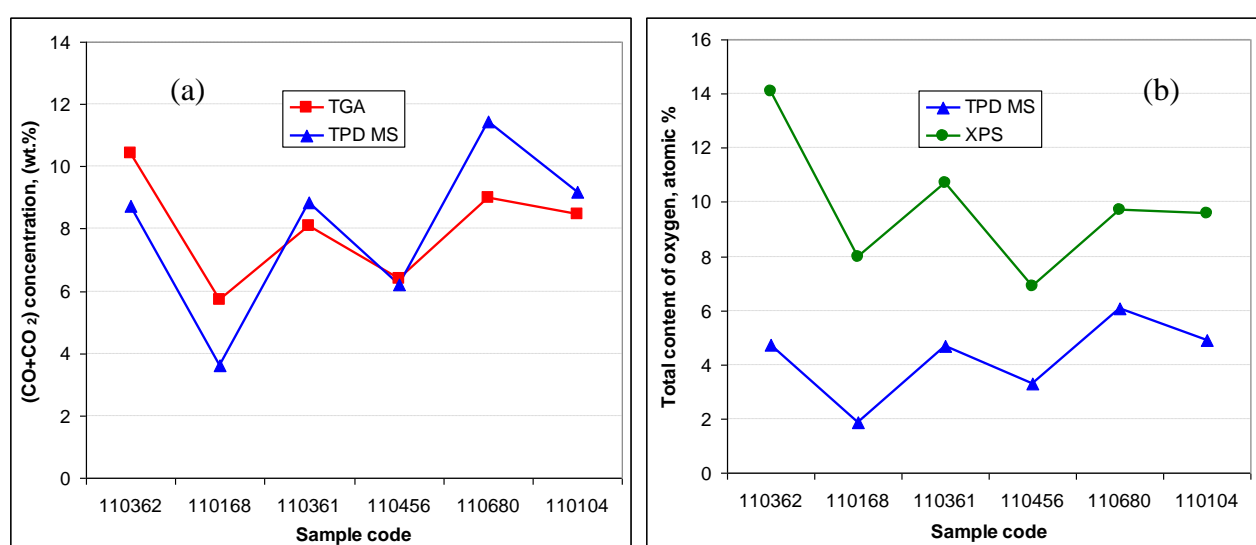


Fig. 11. Concentration of O-content groups (a) and total contents of oxygen on the surfaces of activated carbons (b).

Water vapour adsorption isotherms on the activated carbons. The isotherms of water adsorption on the research activated carbons correspond to type V isotherms [3, 4, 7, 9, 11, 31] (Fig. 12). The water adsorption isotherms begins from an extremely low relative pressure p/p_0 for all samples and have noticeable bulging parts which could be explained by an existence of ultramicroporosity in the carbons or by a significant amount of surface active centers (oxygen functional groups) and the primary water adsorption on them [1, 5, 9]. Then the amounts of water adsorption rise almost linearly with p/p_0 until $p/p_0 = 0.3$. Step increases in adsorption amounts are observed at about $p/p_0 = 0.55\text{--}0.6$. Features of the pore volume filling for each pair of the activated carbons at average relative pressures (the steep rise of the isotherms occurs at approximately the same p/p_0) indicate the similarity of their microporous structures.

The desorption branches for all samples do not overlap with the adsorption ones, giving a representative pronounced hysteresis (Fig. 12). The adsorption and desorption branches of water adsorption isotherms for the microporous carbons (110168, 110456, 110104) come close to each other and give a plateau at high relative pressures. As opposed to this, a gradual rise of water uptake and the existence of wide hysteresis loops at high relative pressures up to $p/p_0 = 0.95$ are observed for the mesoporous carbons (110362, 110361, 110680).

Whereas microporosity of activated carbon is a critical factor which determines the total sorption uptake [32], comparison of the maximum values of water adsorption and the micropore volumes was carried out in the research (Fig. 12).

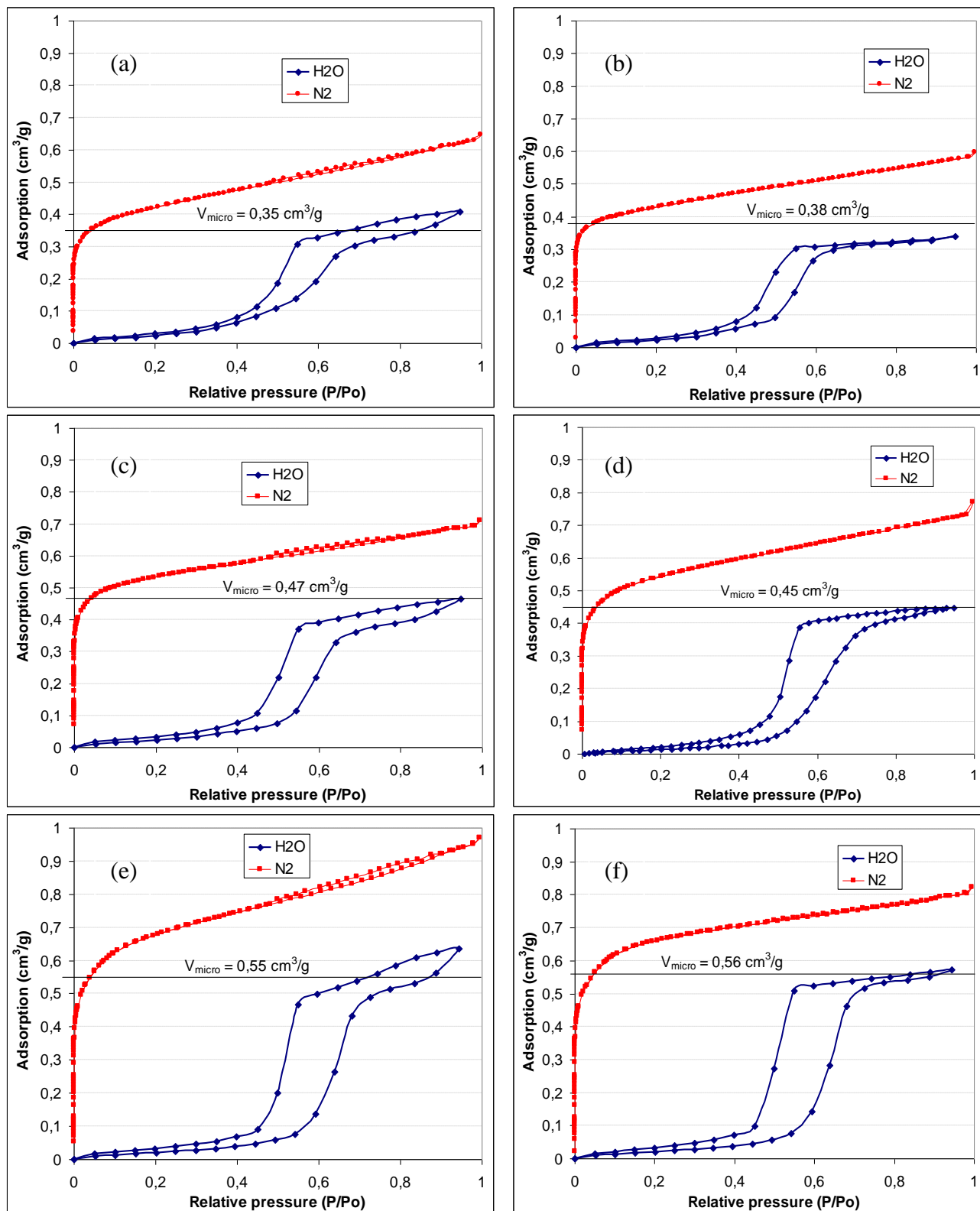


Fig. 12. Uptake of water and liquid nitrogen on the activated carbon samples: 110362 (a), 110168 (b), 110361 (c), 110456 (d), 110680 (e), and 110104 (f).

The water adsorption capacities for the microporous samples are almost equal (or slightly less) to their micropore volumes determined from nitrogen adsorption isotherms, V_{micro} . The maximum values of water adsorption in the case of mesoporous carbons considerably exceed the micropore volumes V_{micro} , and are attributable to the capillary condensation in mesopores [4, 9, 31]. Nevertheless, the total volumes of water uptake both for micro- and mesoporous activated carbons are significantly less than those determined from nitrogen adsorption (Fig. 13). (The values of water adsorption in mesopores, which are presented in the figure, have been determined as a difference

between the volume of micropores and the maximum water adsorption). This could be due to a mechanism of cluster pore filling in which the water density is less than its bulk density [33-36]. Alternatively, it is possible water is not able to condense in the bigger mesopores [37] (Fig. 14).

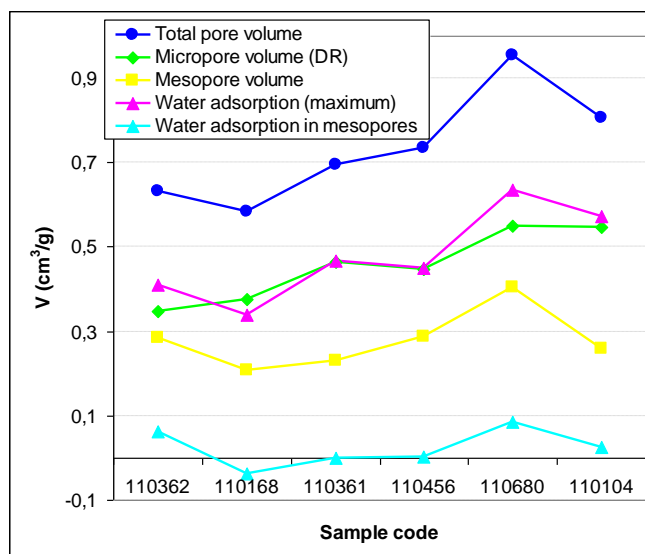


Fig. 13. Comparison of the structural characteristics of the activated carbon samples and the values of water adsorption.

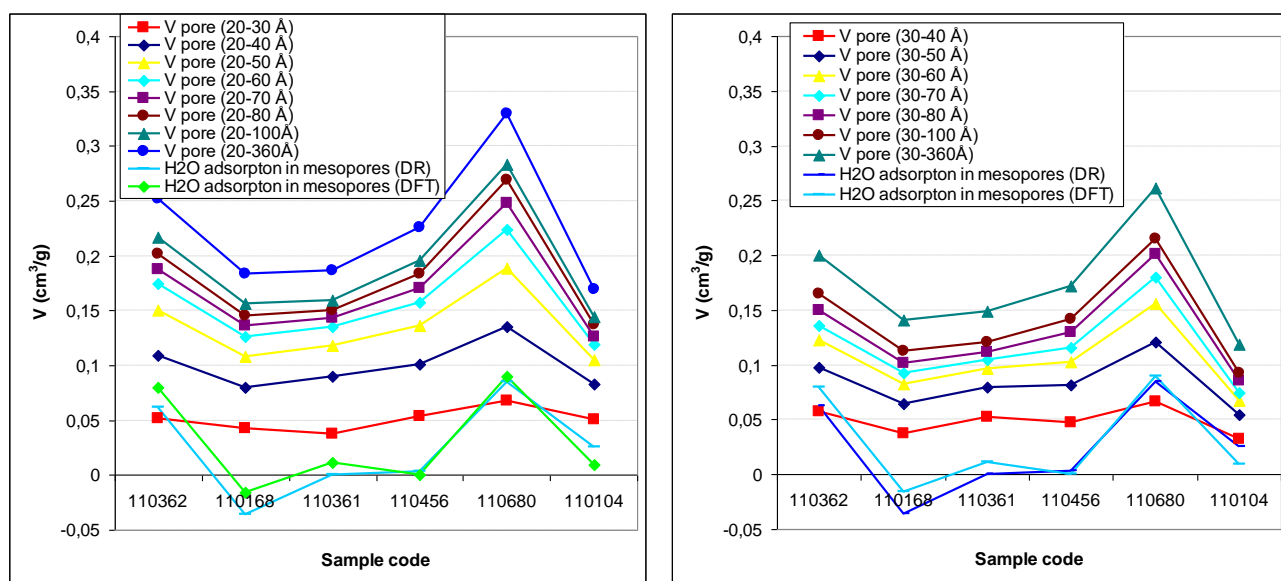


Fig. 14. Comparison of the pore volumes in different size ranges and the values of maximum water adsorption.

The dependence of the maximum water adsorption on the concentration of primary active centers on the surface of the activated carbons is shown in Fig. 15 a. The slope of the line gives the average number of water molecules per one surface active center at $p/p_0 = 1$, which is from 4 (XPS data) to 9.5 molecules (TPD-MS data) per the center.

The adsorption of water vapors on the surface of activated carbon with a relatively high concentration of active centers can take place with the formation of continuous adsorption layer [2, 34]. In this case the value of maximum water adsorption is proportional to the specific surface area of the activated carbon samples (Fig. 15 b). The limiting value of water vapor adsorption per unit of the activated carbon surface area was determined from the slope of dependence of $A_{H_2O_{max}}$ on S_{BET} , and it was about 20 mkmol/m^2 .

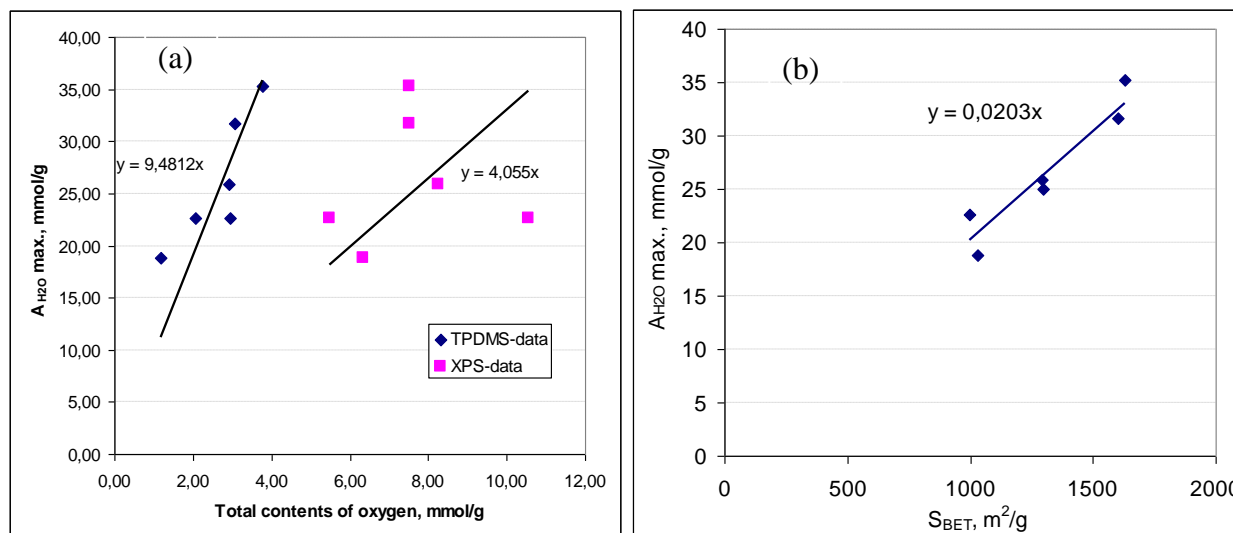


Fig. 15. Values of maximum water adsorption as a function of the amount of primary active centers (a) and the values of surface area for the activated carbon samples (b).

Conclusions

In this work, the correlation between adsorption characteristics of micro- and mesoporous activated carbons towards water and their internal structures defined on the basis of nitrogen and carbon dioxide adsorption isotherms as well as the chemical state of the surface and the nature of primary adsorption sites have been studied.

It has been shown that the water adsorption isotherms at low relative pressures have noticeable bulging parts which could be explained by an existence of ultramicroporosity in the carbons or by a significant amount of surface active centers (oxygen functional groups) and the primary water adsorption on them. The adsorption and desorption branches of water adsorption isotherms for the microporous carbons come close to each other and give a plateau at high relative pressures. The water adsorption capacities for the microporous samples are almost equal (or slightly less) to their micropore volumes determined from nitrogen adsorption isotherms, V_{micro} . As opposed to this, a gradual rise of water uptake and the existence of wide hysteresis loops at high relative pressures up to $p/p_0 = 0.95$ are observed for the mesoporous carbons. Moreover, the maximum values of water adsorption in this case considerably exceed the micropore volumes V_{micro} , and are attributable to the capillary condensation in mesopores. Nevertheless, the total volumes of water uptake both for micro- and mesoporous activated carbons are significantly less than those determined from nitrogen adsorption. This could be due to a mechanism of cluster pore filling in which the water density is less than its bulk density. Alternatively, it is possible water is not able to condense in the bigger mesopores.

References

1. M.M. Dubinin. Water vapor adsorption and the microporous structures of carbonaceous adsorbents. *Carbon* 1980; 18: 335-364.
2. R.Sh. Vartapetyan, A.M. Voloshchuk. The mechanism of the adsorption of water molecules on carbon adsorbents. *Russ. Chem. Rev.* 1995; 64: 985-1002.
3. S.J. Gregg, K.S.W. Sing. *Adsorption, Surface Area and Porosity* (2 ed.). Academic Press, 1982, 303 p.
4. G. Marban, A. Fuertes. Co-adsorption of n-butane/water vapour mixtures on activated carbon fibre-based monoliths. *Carbon* 2004; 42: 71-81.
5. E.A. Muller., F.R. Hung, K.E. Gubbins. Adsorption of water vapor – methane mixtures on activated carbons. *Langmuir* 2000; 16: 5418–5424.

6. J. Pires, M.L. Pinto., A. Carvalho, M.B. Carvalho. Assessment of hydrophobic-hydrophilic properties of microporous materials from water adsorption isotherms. *Adsorption* 2003; 9 (4): 303-309.
7. A.M. Slassi, M. Jorge, F. Stoecki, N.A. Seaton. Water adsorption by activated carbons in relation to their microporous structure. *Carbon* 2003; 41: 479-486.
8. Wood G.O., Lodewyckx P., Correlation for high humidity corrections of rate coefficients for adsorption of organic vapors and gases on activated carbons in air-purifying respirator cartridges, *J. of the Intern. Society of Respiratory Protection* 2002; 58-64.
9. J. Mahle, D. Friday. Water adsorption equilibria on microporous carbons correlated using a modification of the Sircar isotherm. *Carbon* 1989; 27: 835-843.
10. L. Cossarutto, T. Zimny, J. Kaczmarczyk, T. Siemieniowska, J. Bimer, J.V. Weber, Transport and sorption of water vapour in activated carbons. *Carbon* 2001; 39: 2339-2346.
11. A.M. Slassi, M. Jorge, F. Stoeckli, N.A. Seaton. Modelling of water adsorption by activated carbons: effects of microporous structure and oxygen content. *Carbon* 2004; 42 (10): 1947-1952.
12. J.K. Brennan, T.J. Bandosz, K.T. Thomson, K.E. Gubbins. Water in porous carbons. Review in *Colloids and Surfaces A: Phys. and Eng. Aspects* 2001; 187-188: 539-568.
13. K.S.W. Sing, D.H. Everett, R.A.W. Haul, L. Moscou, R.A. Pierotti, J. Rouquerol, T. Siemieniowska. *Pure and Applied Chemistry* 1985; 57 (4): 603-619.
14. P. Kowalczyk, K. Kaneko, L. Solarz, A.P. Terzyk, H. Tanaka, R. Holyst. Modeling of the hysteresis phenomena in finite-sized slitlike nanopores. Revision of the resent results by rigorous numerical analysis. *Langmuir* 2005; 21: 6613-6627.
15. J.J. Freeman, J.B. Tomlinson, K.S.W. Sing, C.R. Theocharis. Adsorption of nitrogen and water vapour by activated Nomex chars. *Carbon* 1995; 33 (8): 795-799.
16. A. Guillot, F. Stoeckli. Reference isotherm for high pressure adsorption of CO₂ by carbons at 273 K. *Carbon* 2001; 39: 2059-2064.
17. J. Jagiello, M. Thommes. Comparison of DFT characterization method based on N₂, Ar, CO₂, and H₂ adsorption applied to carbons with various pore size distributions. *Carbon* 2004; 42: 1225-1229.
18. A.A. Peri-Grujic, O.M. Neskovic, M.V. Veljkovic, M.D. Lausevic, Z.V. Lausevic. A TPD-MS study of glassy carbon surfaces oxidized by CO₂ and O₂. *J.Serb.Chem.Soc.* 2002; 67 (11): 761-768.
19. I. Avraham, A. Danon, J.E. Koresh. Study of carbon molecular sieve fibres by atmospheric TPD-MS of H₂O, CO, CO₂. *J. Chem. Soc., Faraday Trans.*, 1998; 94 (13): 1869-1874.
20. H. Valdes, M. Sanchez-Polo, J. Rivera-Utrilla, C.A. Zaror. Effect of Ozone Treatment on Surface Properties of Activated Carbon. *Langmuir* 2002; 18: 2111-2116.
21. A. Fabregat, C. Bengoa, J. Font, F. Stueber. Reduction, modification, and valorization of sludge: removals. IWA Publishing, London, 2011, 224 p.
22. R.L. Frost, M.L. Weier, Thermal treatment of whewellite - a thermal analysis and Raman spectroscopic study. *Thermochimica Acta* 2004; 409 (1): 79-85.
23. *Surface Analysis: the principal techniques* / ed. by J.C. Vickerman, I.S. Gilmore. (2 ed.) Wiley, 2009, 666 p.
24. *Experimental methods in the physical sciences, Vol. 38: Advances in surface science* / ed. by H.S. Nalwa., Academic press, 2001, 455 p.
25. G.S. Herman, Z. Dohnal'ek, N. Ruzycski, U. Diebold. Experimental Investigation of the Interaction of Water and Methanol with Anatase-TiO₂. *J. Phys. Chem. B* 2003; 107: 2788-2795.
26. S.J. Kerber, J.J. Bruckner, K. Wozniak, S. Seal, S. Hardcastle, T.L. Barr. The nature of hydrogen in x-ray photoelectron spectroscopy: General patterns from hydroxides to hydrogen bonding. *J. Vac. Sci. Technol. A* 1996; 14 (3): 1314-1320.
27. G. Ketteler, P. Ashby, B.S. Mun, I. Ratera, H. Bluhm, B. Kasemo, M. Salmeron. In situ photoelectron spectroscopy study of water adsorption on model biomaterial surfaces. *J. Phys.: Condens. Matter* 2008; 20: 184024-184030.
28. B. Winter, E.F. Aziz, U. Hergenhan, M. Faubel, I.V. Hertel. Hydrogen bonds in liquid water studied by photoelectron spectroscopy. *J. Chem. Phys.* 2007; 126: 124504-124509.

29. M.E. Simonsen, C. Sønderby, Zh. Li, E.G. Søgaard. XPS and FT-IR investigation of silicate polymers. *Journal of Materials Science*. 2009; 44 (8): 2079-2088.
30. Soo-Jin Park, Ki-Seok Kim. Surface Characterization of Carbon Materials by X-ray Photoelectron Spectroscopy. *Microscopy: Science, Technology, Applications and Education A. Mendez-Vilas and J. Diaz (Eds.) FORMATEX 2010*; 1905-1916.
31. T. Matsuoka, H. Hatori, M. Kodama, J. Yamashita, N. Miyajima, Capillary condensation of water in the mesopores of nitrogen-enriched carbon aerogels. *Carbon* 2004; 42: 2329-2366 (2346-2349).
32. T. Bandoz, J. Jagiello, J. Schwarz. Effect of surface chemistry on sorption of water and methanol on activated carbons. *Langmuir* 1996; 12: 6480-6486.
33. D.D. Do, H.D. Do. A model for water adsorption in activated carbon. *Carbon* 2000; 38 (5): 767-773.
34. T. Kimura, H. Kanoh, T. Kanda, T. Ohkudo, Y. Hattori, Y. Higaonna, R. Denoyel, K. Kaneko. Cluster-associate filling of water in hydrophobic carbon micropores. *J. Phys. Chem. B* 2004; 108: 14043-14048.
35. K. Kaneko, Y. Hanzawa, T. Iiyama, T. Kanda, T. Suzuki. Cluster-mediated water adsorption on carbon nanospaces. *Adsorption* 1999; 5: 7-13.
36. T. Ohba, H. Kanoh, K. Kaneko. Cluster-growth-induced water adsorption in hydrophobic carbon nanopores. *J. Phys. Chem. B* 2004; 108: 14964-14969.
37. Y. Hanzawa and K. Kaneko. Lack of a predominant adsorption of water on carbon mesopores. *Langmuir* 1997; 13: 5802-5805.

List of publications, missions and contributions to scientific meetings

1. P. Lodewyckx, N.V. Guzenko, K. László, M. Thommes. The features of water vapour adsorption on micro- and mesoporous activated carbons. Precarb-12, Budapest, Hungary, 15-16 June 2012.

Summary

The correlation between adsorption characteristics of micro- and mesoporous activated carbons towards water and their internal structures defined on the basis of nitrogen and carbon dioxide adsorption isotherms as well as the chemical state of the surface and the nature of primary adsorption sites have been studied in the research.

It has been shown that the water adsorption isotherms at low relative pressures have noticeable bulging parts which could be explained by an existence of ultramicroporosity in the carbons or by a significant amount of surface active centers (oxygen functional groups) and the primary water adsorption on them. The adsorption and desorption branches of water adsorption isotherms for the microporous carbons come close to each other and give a plateau at high relative pressures. The water adsorption capacities for the microporous samples are almost equal (or slightly less) to their micropore volumes determined from nitrogen adsorption isotherms, V_{micro} . As opposed to this, a gradual rise of water uptake and the existence of wide hysteresis loops at high relative pressures up to $p/p_0 = 0.95$ are observed for the mesoporous carbons. Moreover, the maximum values of water adsorption in this case considerably exceed the micropore volumes V_{micro} , and are attributable to the capillary condensation in mesopores. Nevertheless, the total volumes of water uptake both for micro- and mesoporous activated carbons are significantly less than those determined from nitrogen adsorption. This could be due to a mechanism of cluster pore filling in which the water density is less than its bulk density. Alternatively, it is possible water is not able to condense in the bigger mesopores.

Keywords: activated carbons, pore structure characterization, nitrogen adsorption, surface chemistry, primary adsorption centre, Thermogravimetric Analysis, X-ray Photoelectron Spectroscopy, Temperature-Programmed Desorption / Mass-Spectrometry, water vapour isotherm